Modeling the Effect of Channel Bends on Microfluidic Flow

Jianliang You, Luis Flores, Muthukumaran Packirisamy, Ion Stiharu
Micromechatronics Lab, CONCAVE Research Centre
Department of Mechanical and Industrial Engineering
Concordia University
1455 de Maisonneuve Blvd. West, Montreal, Quebec, H3G 1M8
CANADA

Abstract: The bends of different angles have many applications in microfluidic applications and it is very important to understand the flow behavior in these microbends. This paper presents the modeling of the flow behavior in micro bends of various angles in order to meet with implementation of expected flow behavior. As the sharp-angle-bends are very rare in actual applications due to their higher pressure loss and disturbance to the original laminar flow, this paper presents the results on analysis of microchannel with different bend angles. A series of rectangular microchannels with the dimensions in the range of 200μm and with the bend angles of 45°, 60°, 75°, 90°, 120°, 135°, 150° and 180° have been modeled using finite element method. The fluid characteristics such as flow rate and pressure loss have been established. The results also show that the flow separation and recirculation occur when the flow passes through the convex corner of the bend and becomes more critical as the bend angle decreases. The results also show the presence of flow oscillations along the channel under certain conditions.

Key-Words: Microfluidics, Microchannels, Microbends, MEMS, Flow Oscillations

1 Introduction

More and more innovated microfluidic systems and components have been created and found to have very vast applications in further academic research, industrial and medical fields, owing to the rapid development of micromachining. Typical applications of these microfabricated fluidic systems include biological and chemical sensing and analysis, mass transportation or delivery, molecular separation, mixing, reaction, DNA sequencing and synthesis, environmental monitoring and so on. Microchannels are indispensable passages for fluid and thus basic components in all microfluidic or microfluidic-related chips. Many studies have been conducted to analyze the behavior of microchannel flows. However, since the ability to fabricate micro scale fluidic devices is relatively new, still little is known about the flow behavior in such a minute channel or passage. The disputes on discrepancies between micro-scale flow and macro-scale Stokes flow theory have been kept going. And some previously unnoticed phenomena such as flow separation, or recirculation at around a sudden turning corner or a sudden constriction or enlargement section of microchannels due to geometric or dynamic causes, have been observed. This separation will apparently contract the original cross-section area to a relatively smaller equivalent value, thus increase the resistance of the passage to the flow. In addition, the negligible flow separation under relatively low velocity or in a laminar flow will gradually grow up along the transition after the corner or constriction, and disturb to transform the local flow of a certain region into a turbulent status.

Flow through a straight channel is the simplest but most common case in microfluidic-related systems. Flow behavior of such channels has been vastly analyzed and tested. The obtained results show that anomalous behaviors in a microchannel flow (compared with those of macro channels) have come from the relatively larger influence of surface roughness on the flow, and highly experimental uncertainties due to the micro dimensions [1]-[8]. However, arrangements of channel bends or curves, expansions or contractions, constrictions, and various shapes of

inlets and outlets are also very common in practice due to the design and technological constraints or limitations. Any of these local transitions of passages will cause a sudden change to flow velocity or pressure gradient, resulting in more or less pressure loss to the whole microfluidic system. S. Y. K. Lee, et al [9], has conducted an experiment on a channel with a 90° bend and channel dimensions of 20μm×1.1μm×5810μm. The results showed that flow separation occurred at the turning corners and testified a pressure drop at the bend location (see Fig. 1).

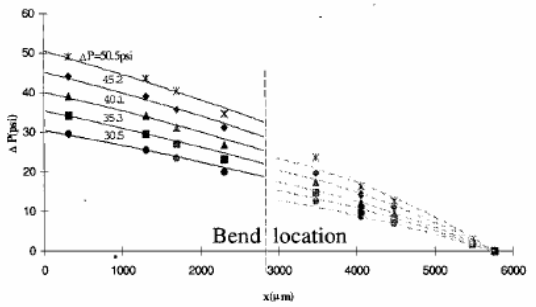

Fig. 1 Pressure Drop in a 90°-Bend Channel [9]

Moreover, Wing, et al [10] has constructed an experimental device to test the effect of constriction with sharp corners in the fluid stream. Nitrogen gas was driven to pass through the microchannel. The mass flow rates measured seem a nonlinear function of the pressure drop and a monotonic decrease of the flow rate with decreasing constriction-gap width was observed. The pressure distribution along the microchannel showed a step pressure drop across the constriction element. Both mass flow rate and pressure measurements indicate that flow separation from the constriction sharp corners occurs (see Fig. 2).

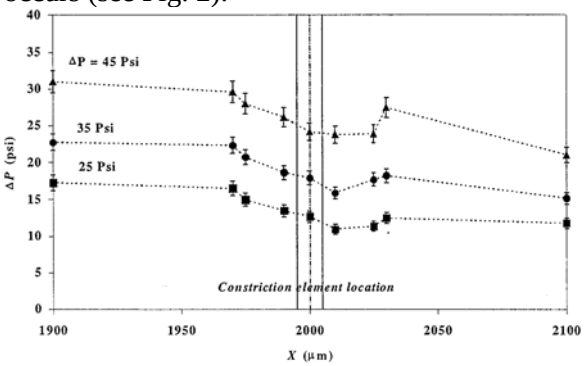

Fig.2 Pressure Drop along Constriction [10]

Reni Raju and Subrata Roy [11] presented a hydrodynamic model to simulate the gas flow through a micro-column with two sharp 90-deg bends for a maximum Reynolds number of 0.04. Using both no-slip and first-order slip boundary conditions, they concluded that the twisted geometry reduces the mass flow rate by up to 160% than that of a straight microchannel with the same overall dimensions. Velocity solutions also predict small recirculations at bends (see Fig. 3).

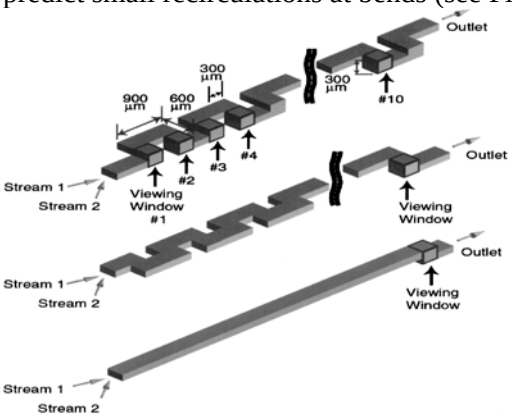

Fig. 3 Microchannels with/without 90° Bends [11]

Masaya Kakuta, et al [12] has given a brief description on the development of micro-fabricated devices for fluid mixing. In order to obtain a homogenously fluid from mixing of different fluids, microchannels with certain angle bends are basic components in fulfillment of the required task. The flow can be laminar flow or turbulent flow. The proper layout design of microchannels proves being very efficient in mixing. Microfluidics often involves in practice extremely low Reynolds number, such that the flow usually belongs to the laminar regime. Thus there appear designs of serial lamination or parallel lamination with serpentine curves or bends. Paul J. A. Kenis, et al[13] even utilize multiphase laminar flow to construct micro reactors inside capillaries thus to form expected patterns of microfluidics.

Compared with fluid mechanics of macroscale, relatively few studies have focused on various geometric arrangements for microchannel flow. Thus our current understanding to these micro-flow behaviors is far from sufficiency. Only limited prior work has appeared in the literature exploring pressure-driven liquid flows through crooked microchannels. It is therefore necessary to carry out computer simulations under various

conditions or cases at first, avoiding repeated constructions of unnecessary experimental establishment. The objective of this paper is to numerically calculate the characteristics of water flow in a series of microchannels with different bend angles, and to explain or analyze the simulation results.

2 Numerical Analysis

2.1 Model Descriptions

2.1.1 Reynolds Number

Laminar flow provides a means by which particles or molecules can be transported in a relatively predictable manner through channels. For flows in microchannels of certain cross sections, the Reynolds number can be used to judge whether the flow is turbulent or laminar. The Reynolds number is given by

$$\mathrm{Re} = \frac{\rho D_h u}{\eta} = \frac{D_h u}{\nu} \qquad (1)$$

where u is the average velocity in the channel, ν and $\boldsymbol{\rho}$ are the kinematic viscosity and density of the fluid, D_h is perimeter of the cross-section. The transition from complete laminar flows to fully turbulent flows in micro channels starts from Reynolds numbers of 400 to 2000. This transition decreases to the lower value for micro-channels with smaller hydraulic diameters (For example, Re=500 when D_h=9.7 μm and 6.9 μm). In our work, Re<400 is accepted as laminar flow; 400<Re<1000 is the transition region and Re>1000 is accepted as fully turbulent flow. Different critical Reynolds numbers result from many factors such as the shape and aspect ratio of channel cross-section, and surface roughness.

2.1.2 Hydraulic Diameter

In consideration of anisotropic silicon etching and isotropic etching in micromachining, only several common shapes of cross section are chosen for fabrication of microchannels, such as rectangular, rounded rectangular, trapezoidal, triangular cross sections. In this simulation, we choose a rectangular channel as our model.

The hydraulic diameter D_h can be used to assess flows through completely filled channels as well as those that are only partially filled. It is written as

$$D_h = \frac{4 \times Cross\ Section\ Area}{Wetted\ Perimeter} = \frac{4A}{P_{wet}} \qquad (2)$$

The term “wetted perimeter” refers to the perimeter of the channel that is in direct contact with the flow. For channels that are fully filled, the wetted perimeter is simply the perimeter of the cross sectional area of the channel. With given width a and thickness b of our rectangular cross-section, D_h can be easily written as $2ab/(a+b)$.

2.1.3 Model Set-up

Focusing on the analysis of laminar distilled water flow through crooked or bended silicon microchannels, we assume conditions and denotations shown below:

Steady-state, incompressible Newtonian, iso-thermal flow, with a laminar fully developed velocity profile, also with constant fluid physical properties, and with all rigid and nonporous channel walls, is considered.

Instead of straight microchannels, here we choose a series of angles of channel bends with the same rectangular cross-section and length dimensions: 60°, 90°, 120°, 150°, and 180° bends, which we will encounter in our designs under some structural and machining limitations.

Thus the model we chose is 90 μm ×10 μm in cross-section and 200 μm +200 μm in length. The hydraulic diameter is calculated as 18 μm. The calculated Reynolds number is far more less than 1.

2.2 Numerical Analysis

Microfluidic devices usually operate in regimes where the flow moves slowly. To determinate whether a flow is slow relative to its length’ scale, we need to scale the original dimensions to their relative sizes. If we set D and u as the characteristic size and average velocity respectively, then

$$x_i^* = \frac{x_i}{D} \quad u_i^* = \frac{u_i}{u} \quad t^* = \frac{t}{D/u} \quad p^* = \frac{p}{\eta u / D}$$

thus

$$x_i = D \cdot x_i^* \quad u_i = u \cdot u_i^*$$
$$t = (D/u).t^* \quad p = (\eta u / D).p^* \qquad (3)$$

The starred quantities are then dimensionless quantities whose size varies from zero to the order of one. After substituting these expressions, the Navier-Stokes equations can be simplified to:

$$\mathrm{Re}\left(\frac{\partial u_i^*}{\partial t^*}+u_j^*\frac{\partial u_i^*}{\partial x_j^*}-\frac{F_i D}{u^2}\right)=-\frac{\partial p^*}{\partial x_i^*}+\frac{\partial^2 u_i^*}{\partial x_j^{*2}}$$

$$\frac{\partial u_i^*}{\partial x_i^*}=0 \qquad (4)$$

in which all of the variables and terms are dimensionless forms. If the Reynolds number is very small, as in our case, $\mathrm{Re}<<1$, then the left side becomes negligible, leaves only

$$0=-\frac{\partial p^*}{\partial x_i^*}+\frac{\partial^2 u_i^*}{\partial x_j^{*2}}$$

$$\frac{\partial u_i^*}{\partial x_i^*}=0 \qquad (5)$$

as the governing equations, which can be further written as:

$$\frac{\partial^2 u}{\partial x^2}+\frac{\partial^2 u}{\partial y^2}=\frac{1}{\eta}\frac{dp}{dz} \qquad (6)$$

Before proceeding to the case of a channel bend, we first consider the laminar flow of a straight rectangular channel. Analytical solution to the partial differential equations under a rectangular cross section is derived:

$$u(y,z)=\frac{16a^2}{\eta\pi^3}\left(-\frac{dp}{dx}\right)\cdot$$

$$\sum_{i=1,3,5,\ldots}^{\infty}(-1)^{(i-1)/2}\left[1-\frac{\cosh(i\pi z/2a)}{\cosh(i\pi b/2a)}\right]\frac{\cos(i\pi y/2a)}{i^3}$$

$$\dot{Q}=\frac{4ba^3}{3\eta}\left(-\frac{dp}{dx}\right)\left[1-\frac{192}{\pi^5 b}\sum_{i=1,3,5,\ldots}^{\infty}\frac{\tanh(i\pi b/2a)}{i^5}\right]$$

where *a* and *b* are half width and half thickness of the cross-section, ρ,η are the density and dynamic viscosity of the fluid, respectively.

And a simplified solution for the correlation of pressure drop Δp and friction factor *f* of the channel can be shown as

$$\Delta p=4f\frac{L}{D_h}\rho\frac{U^2}{2} \qquad (7)$$

where *U* is the mean fluid velocity at the cross-section of the microchannel and L is the z-directional length along the channel. For fully developed laminar flows in parallel (*s* denotes spacing) plates, there is an exact solution to the Navier-Stokes equations. The resulting velocity profile is parabolic and

$$f=24/\mathrm{Re},\ D_h=2s \qquad (8)$$

where *f* is also called the Fanning factor.

For fully developed laminar flows in rectangular cross-section channels,

$$f=(24/\mathrm{Re}).(1-1.3553r+1.9467r^2 -1.7012r^3+0.9564r^4-0.2537r^5) \qquad (9)$$

where aspect ratio $r<1$. This result shows that the Fanning factor for rectangular channels should be modified by a polynomial function of the aspect ratio of the channel.

Unlike solutions in fully developed laminar straight channel flow, hydrodynamic behavior around and slightly after the channel bend is more complex because of the secondary flows induced by suddenly changed channel walls. If we denote ϕ as a channel bend angle, then pressure drop along this local bend has some kind of relationship with the angle, i.e.,

$$\Delta p=k\ f\ k_\phi(\phi)\ k_u(U^2) \qquad (10)$$

where k is a constant value; f is a properly modified Fanning factor under certain conditions and Reynolds number; k_ϕ is a function of bend angle of the crooked channel; and k_u is a function of average flow velocity square.

Actually, in microfluidic applications, what one needs to quantify is the flow properties on inlet and outlet sections of the microchannel with bends. No matter what kind of flow it may be inside the short section of the bend, the flow in other major straight sections of the channel is usually laminar and thus more useful in practice. Equations on laminar straight channel flow can hence be applied on two ends of the channel. Simply, in an incompressible fluid with no slip boundary, the Bernoulli equation can therefore be used to describe the flow in the inlet and outlet:

$$\frac{V^2}{2g}+z+\frac{p}{\rho g}=C \qquad (11)$$

where *z* is the elevation of a point, *V* is the average velocity of the inlet or outlet, *C* is a constant.

However, the velocity profile along the cross-sections of inlet and outlet is important in microfluidic analysis. Generally, this field is still a parabolic kind, which is presented by [19]:

$$\frac{u}{u_{\max}} = [1-(\frac{x}{a})^m][1-(\frac{y}{b})^n] \qquad (12)$$

The integrated form on cross-section is given as:

$$\frac{u}{U} = (\frac{m+1}{m})(\frac{n+1}{n})[1-(\frac{x}{a})^m][1-(\frac{y}{b})^n] \quad (13)$$

where *a, b* are half width and half thickness of the channel, *u* is the velocity at a point and *U* is mean velocity of the cross-section.

For $r<=1/3$, $m = 1.7 + 0.5r^{-1.4}$ and $n=2$.

3 FEM Simulations

3.1 Some Settings in FEMLAB

Constants: Some known constants such as density and dynamic viscosity of the fluid and sometimes the maximum velocity are filled in the form.

Inflow/Outflow Velocity: At inlet boundary, the fluid's velocity is specified by (u_0, v_0, w_0) in 3D. Here z-directional velocity (along the channel) is predefined by the equation (13).

Slip and No-slip: A slip condition means that the normal component of the velocity is zero and that the tangential component of the viscous force vanishes. A no-slip condition means that the fluid's velocity equals that of the boundary, which is usually zero. It is normally to use this condition for all walls.

Normal Flow or Pressure: At a straight-out outflow boundary, the pressure is zero, as are the tangential components of the velocity. Further, the normal component of the viscous force is zero.

Geometric Set-up: Two geometric models are shown in Fig. 4 (after meshed). For the 60°-bend channel, a symmetric dimension is set around the corner. Length of the shorter edge of the channel is 200 μm, half of the total length.

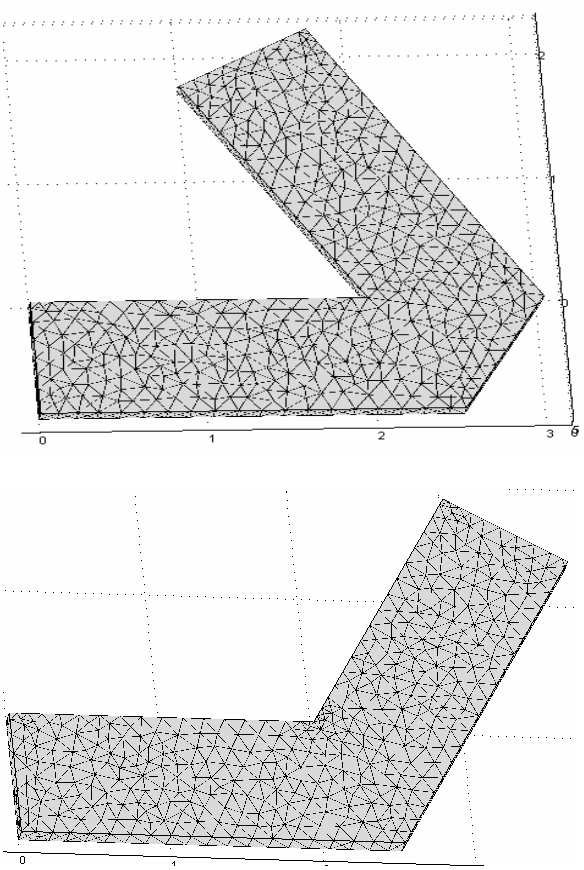

Fig. 4 Geometric Models (after meshed)

Meshing: Even construction of geometry can be considered as an easy task, where seems more complex to get correct meshing. The automatic meshing of the program allows to modify the mesh according to the required analysis. For example, for an analysis at low applied pressure and a smooth channel, non complex mesh gives immediate results, but that is not the case when the pressure is increased. In that case, configuration of the fluid behavior requires dense meshing, especially where the boundary has sudden changes, as in the case of the 60° degree bend.

3.2 3D Simulation Results

Once all settings have been properly done, the mesh design can be followed and tuned. One may consider a finer mesh on the turning convex point, avoiding any diverse problem as aforementioned.

In our simulations, different pressure drops between inlet and outlet of microchannels are

assumed by simply applying the value of the pressure drop on the inlet cross-section and setting the relative outlet pressure to be zero. Then we can derive the corresponding average velocities by boundary integration. Table 1 and 2 show the simulated results.

Table 1 Average Flow Velocities with Bends

Pressure Drop (psi)	Bend Angle	U(μm/s)
2	60°	32.0
2	90°	32.6
2	120°	34.1
2	150°	36.0
2	180°	38.4

Table 2 Average Flow Velocities with Bends

Pressure Drop (psi)	Bend Angle	U(μm/s)
10	60°	160.0
10	90°	163.3
10	120°	170.2
10	150°	179.4
10	180°	192.0

Fig.5 to 10 illustrate the simulated visual results.

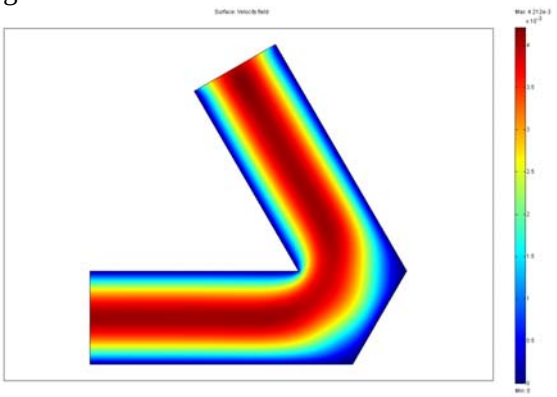

Fig. 5 The 60° Bend Channel

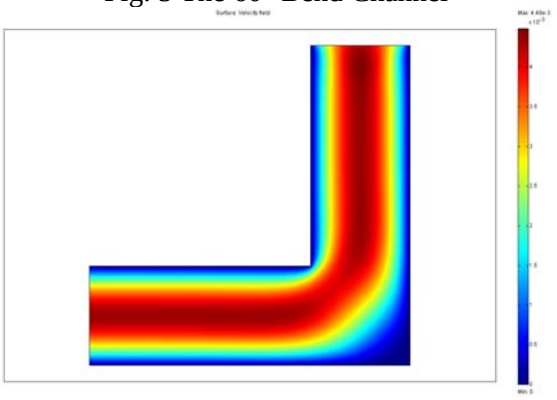

Fig. 6 The 90° Bend Channel

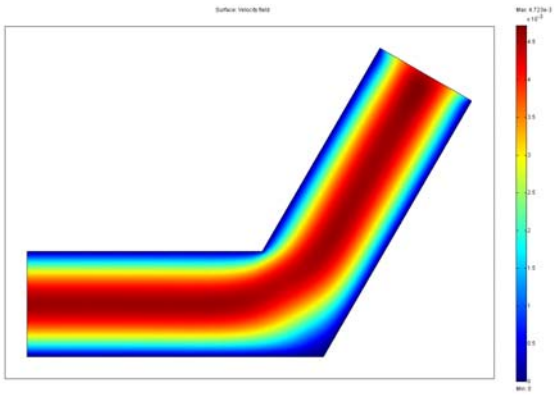

Fig. 7 The 120° Bend Channel

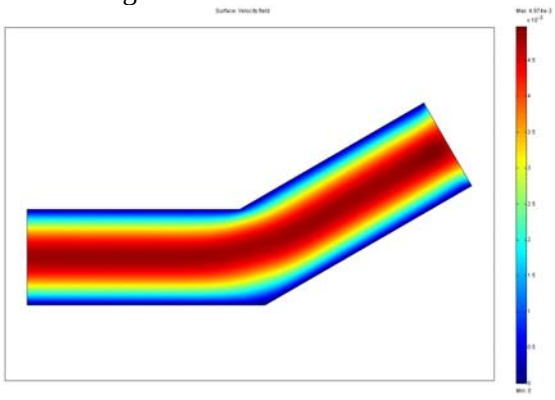

Fig. 8 The 150° Bend Channel

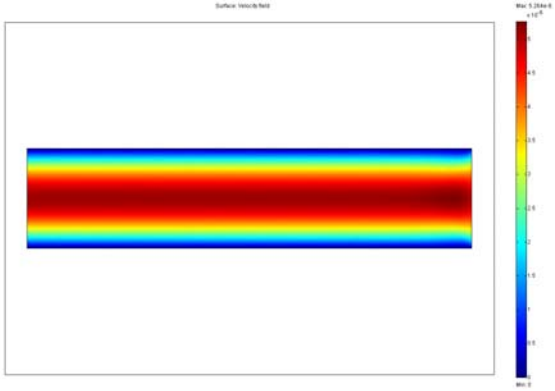

Fig. 9 The 180° Bend (straight) Channel

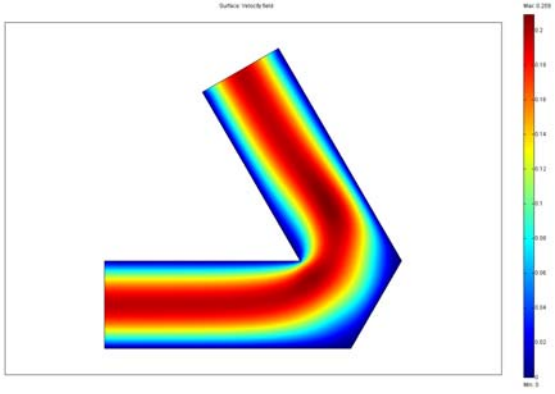

Fig. 10 Higher Pressure Applied

These visual results are in accordance with both practical observations and analytical solutions. Velocity field at the cross-section is of parabolic kind, with the maximum velocity at the central streamline. As can be seen from the figures, flows around and after bends have a gradual change of velocity field. As the angle of the bend becomes sharper, the change in the velocity field occurs more suddenly and the period of recovery becomes longer. Moreover, as the bend angle becomes smaller, the central stream line moves closer to the convex corner wall whereas velocity at concave corner seems almost zero. In addition, when a higher pressure is applied on the fluid, the central stream line after the corner will move beyond the geometric central line and return to it after some transitional distance. Due to the extremely low Reynolds number, laminar flow is kept even under a higher drive pressure and with a sharp angle bend.

The resulted velocities from Table 1 and Table 2 for different bend angles under two different pressure drops can be used to draw some curves like the ones in Fig. 11 and Fig. 12.

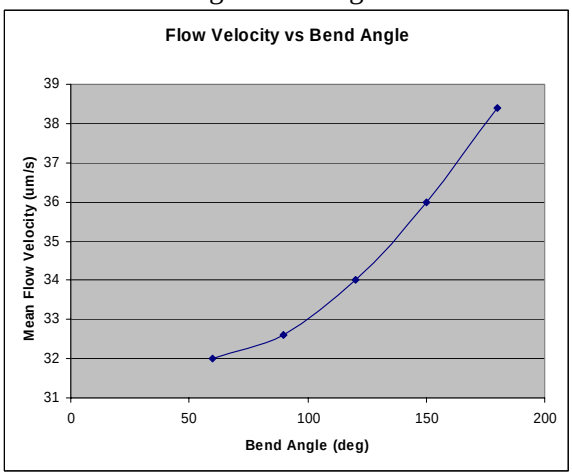

Fig. 11 Curve of Velocity and Bend Angle

These two curves tell us that mean flow velocity increases as the bend angle increases. There is a certain exponential relation between velocity and bend angle no matter what drive pressure is applied on the flow. We notice that there exists a small amount of velocity difference between 60° bend and 90° bend. This result may come from modified symmetric concave corner of 60° bend. The derivative is larger when bend angle continues to increase after 90°. But if bend angle goes beyond 180°, the curve will go down to repeat geometrically symmetric process.

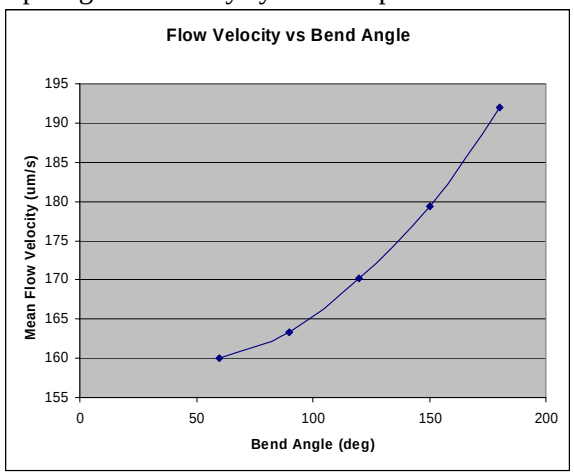

Fig. 12 Curve of Velocity and Bend Angle

4 Some Conclusions

In order to better understand microfluidics phenomena, it is necessary to further explore fluidic mechanics in both micro-scale and nano-scale. Still, as the dimension comes beyond micro world, Navier-Stokes theory becomes unable. However, considering combinational effects of various factors such as wall roughness, aspect ratio of cross-section, channel geometric arrangement (bend angle, geometrics of turning corner, expansion, constriction, contraction and so on), fluid property, and applied forces, traditional theory still plays an important role in microfluidic analysis.

Some conclusion points can be drafted from this simulation work:

1) Reynolds number is still a critical parameter to be considered in fluidic research even for the flow through very small microchannels.

2) Proper geometric arrangement of channels is important in microfluidic applications. Though straight channel is a basic conduit element, other types of channels for fluid transportation such as right, obtuse or even sharp angle bends with occasionally rounded corners, are also common in microfluidic chips.

As is often the case, all channels in the same fluidic system should better be arranged in the same elevation, thus to avoid the complex issues that are associated with the gravity flow.

Due to some limitations resulting from some fabrication and required structures, bends of channels will sometimes be used. Even in this case we still can reach a smaller pressure loss by setting a properly fillet at the bend corner.

3) Specific conditions for flow separation and recirculation should be known to us when we design for a complete laminar flow system. However, as mentioned, microfluidics seldom encounters turbulent flow but emphasizes its attention on transition between fully laminar flow and fully turbulent counter.

Acknowledgement: The supprot of NSERC and NATEQ of this work is acknowledged.

References:

[1] C. M. Ho and Y. C. Tai, Micro-Electro-Mechanical Systems(MEMS) and Fluid Flows, *Annual Review of Fluid Mechanics*, Vol. 30, 1998, pp. 579-612.

[2] Nam-Trung Nguyen & Steven T. Wereley, Fundamentals and Applications of Microfluidics, Artech House, 2002.

[3] Bastian K., Sarah Pedersen, Frederic Ronne Petersen, Institute of Micro and Nanotechnology Center (MIC), Technical University of Denmark, Jan. 2004.

[4] Xu B., Ooi K. T., Wong N. T., and Choi W. K., Experimental Investigation of Flow Friction for Liquid Flow in Microchannels, *Int. Commun. Heat Mass Transfer*, Vol. 27, 2000, pp. 1165–1176.

[5] Judy J., Maynes D., and Webb B. W., Characterization of Frictional Pressure Drop for Liquid Flows Through Microchannels, *Int. J. Heat Mass Transfer*, Vol. 45, 2002, pp. 3477–3489.

[6] Wu H. Y., and Cheng P., Friction Factors in Smooth Trapezoidal Silicon Microchannels with Different Aspect Ratios, *Int. J. Heat Mass Transfer*, Vol. 46, 2003, pp. 2519–2525.

[7] J. Koo, C. Kleinstreuer, Viscous Dissipation Effects in Microtubes and Microchannels, *Int. J. Heat Mass Transfer*, Vol. 47, 2004, pp. 3159-3169.

[8] H.Y. Wu, Ping Cheng, Friction Factors in Smooth Trapezoidal Silicon Microchannels with Different Aspect Ratios, *Int. J. Heat Mass Transfer*, Vol. 46, 2003, pp.2519-2525.

[9] S. Y. K. Lee, et al, Microchannels in Series with Gradual Contraction/Expansion, *Proc. Int. Mech. Eng. Congress & Exposition, MEMS*, Vol. 2, 2000, pp. 467-472.

[10] Wing Yin Lee, et al, Pressure Loss in Constriction Microchannels, *J. MEMS*, Vol. 11, No. 3, 2002, pp. 236-244.

[11] Reni Raju and Subrata Roy, Hydrodynamic Model for Microscale Flows in a Channel With Two 90 deg Bends, *J. Fluids Engineering*, Vol. 126, 2004, pp. 489-492.

[12] Masaya Kakuta, et al, Microfabricated Devices for Fluid Mixing and Their Application for Chemical Synthesis, *The Chemical Record*, Vol. 1, 2001, pp. 395-405.

[13] P. J. A. Kenis, et al, Microfabrication Inside Capillaries Using Multiphase Laminar Flow Patterning, *Science*, Vol. 285, 1999, pp. 83-85.

[14] Peng X. F., Peterson G. P., Wang B. X., Frictional Flow Characteristics of Water Flowing Through Microchannels, *Experimental Heat Transfer*, Vol. 7, 1994, pp 249-264.

[15] Wu P., Little W. A., Measurement of Heat Transfer Characteristics of Gas Flow in Fine Channel Heat Exchangers Used for Micro-miniature Refrigerators, *Cryogenics*, Vol. 24, No.8, 1984, pp. 415-420.

[16] Choi S. B., Barron R. F., Warrington R. O., Liquid Flow and Heat Transfer in Microtubes, *Micromechanical Sensors, Actuators and Systems*, ASME DSC, Vol. 32, 1991, pp. 123-128.

[17] W. L. Qu, Gh. Mohiuddin Mala, D. Q. Li, Pressure-Driven Water Flows in Trape-Zoidal Silicon Microchannels", *Int. J. Heat and Mass Transfer*, Vol. 43, 2000, pp.353-364.

[18] Hirofumi, et al, Observation of Fluidic Behavior in a Polymethylmethacrylate-Fabricated Microchannel by a Simple Spectroscopic Analysis, *Lab Chip*, Vol. 2, 2002, pp. 8-10.

[19] Hojoon Park, et al, Fabrication of a Microchannel Integrated with Inner Sensors and the Analysis of its Laminar Flow Characteristics, Sensors and Actuators (A), Vol. 103, 2003, pp. 317-329.